Scientia Horticulturae 162 (2013) 125–134

Contents lists available at ScienceDirect

Scientia Horticulturae

journal homepage: www.elsevier.com/locate/scihorti

A model approach revealed the relationship between banana pulp acidity and composition during growth and post harvest ripening

Audrey Etienne [a], Michel Génard [b], Doriane Bancel [b], Sophie Benoit [a], Christophe Bugaud [a,*]

[a] Centre de Coopération International en Recherche Agronomique pour le Développement (CIRAD), UMR QUALISUD, Pôle de Recherche Agronomique de Martinique, BP 214, 97 285 Lamentin Cedex 2, France
[b] INRA, UR 1115 Plantes et Systèmes de Cultures Horticoles, F-84914 Avignon, France

ARTICLE INFO

Article history:
Received 14 May 2013
Received in revised form 5 August 2013
Accepted 8 August 2013

Keywords:
Musa
Organic acids
Mineral elements
Cultivars
Titratable acidity
pH

ABSTRACT

Titratable acidity and pH are important chemical traits for the organoleptic quality of banana since they are related to the perception of sourness and sweetness. Banana fruit has the particularity of having separate growth and ripening stages, during which pulp acidity changes. A modeling approach was used to understand the mechanisms involved in changes in acidity during pulp growth and post harvest ripening. Changes in pH and titratable acidity were modeled by solving a set of equations representing acid/base reactions. The models were built using data from growth and post harvest ripening of three dessert banana cultivars with contrasting acidity. For each model, calculated values were compared to observed values. These models allowed the prediction of pH (R^2 = 0.34; RMSE = 0.75, biais = 0.05) and of titratable acidity (R^2 = 0.81, RMSE = 2.05, biais = −1.44) during fruit growth and post harvest ripening. The sensitivity analyses showed that among acids, malic, citric and oxalic acids are the main contributors to banana pulp acidity, and that among soluble minerals, potassium also plays an important role. Studying the factors that affect the accumulation of organic acids (citric, malic, and oxalic acids) and potassium in banana pulp could be a relevant area of research with the objective of modifying banana fruit acidity.
© 2013 Elsevier B.V. All rights reserved.

1. Introduction

Fruit acidity is a topic of primary importance in improving fruit quality since it influences the perception of both sourness and sweetness (Bugaud et al., 2011; Esti et al., 2002). These two attributes are major drivers of consumer preferences for fruit (Lyon et al., 1993), and are thus important traits to consider in breeding programs. Understanding the elaboration of fruit acidity is also important because acidity controls numerous enzyme activities (Madshus, 1988).

Fruit acidity is commonly measured using two chemical parameters: titratable acidity (TA) i.e. the amount of weakly bound hydrogen ions that can be released from the acids, and pH, the activity of free hydrogen ions. Fruit acidity is due to the acidity of the vacuole which represents about 90% of the volume of most mature fruit cells (Etxeberria et al., 2012). The acidity of the vacuole is the result of its ionic composition, mainly organic acids and mineral cations that determine the vacuolar pH and TA (Etienne et al., 2013). Banana pulp contains three major organic acids, malic acid, citric acid, and oxalic acid, whose concentrations undergo marked changes during growth and ripening (John and Marchal, 1995; Jullien et al., 2008) and phosphoric acid (Bugaud et al., 2013). Banana pulp contains soluble minerals, mainly potassium (K), and to a lesser extent magnesium (Mg), calcium (Ca), and chloride (Cl) (John and Marchal, 1995). During post harvest ripening, mineral content can still change due to migration between the peel and the pulp (Izonfuo and Omuaru, 1988).

There are considerable differences in pH and TA among dessert banana cultivars and among post-harvest ripening stages (Bugaud et al., 2013; Chacón et al., 1987), and the origins of these differences remain unclear. Quantifying the relations between pulp acidity and pulp ionic composition using a modeling approach, would advance our understanding of the determinants of banana acidity. Models of pH and TA predictions have been developed for peach (Lobit et al., 2002) and proved to be powerful tools to understand the mechanisms underlying changes in acidity during peach development. The objective of the present work was to apply and validate these models on banana fruit, in which other ionic species than those

Abbreviations: TA, titratable acidity; RMSE, root mean squared error; K, potassium; Mg, magnesium; Ca, calcium; Cl, chloride; P, phosphorus; IDN 110, Indonesia 110; JB, Pisang Jari Buaya; PL, Pisang Lilin; FW, fresh weight; mEq, milliequivalents; LMM, linear mixed model; SI, sensitivity index.

* Corresponding author. Tel.: +33 5 96 42 30 98; fax: +33 5 96 42 30 01.
E-mail addresses: bugaud@cirad.fr, christophe.bugaud@cirad.fr (C. Bugaud).

0304-4238/$ – see front matter © 2013 Elsevier B.V. All rights reserved.
http://dx.doi.org/10.1016/j.scienta.2013.08.011

found in peach need to be taken into account, and to throw light on the determinants of the changes in pH and TA that occur during the life of the banana pulp, i.e. from growth on the plant through post harvest ripening.

2. Materials and methods

2.1. Model development

2.1.1. pH model

The model used for pH prediction was adapted from Lobit et al. (2002). Banana pulp can be considered as a concentrated aqueous solution of weak acids, mainly malic, citric, oxalic and phosphoric acids, and mineral cations, mainly potassium, magnesium, calcium and chloride. Other acids can be found in banana pulp but were not taken into account in the present study. Weak acids are partly in free form and partly dissociated to form salts with monovalent cations. Proton exchange reactions occur between acids and bases until equilibrium state is reached, which determines the pH and the concentrations of all ionic species. So, to predict the pH of banana pulp solution, the concentrations of the different chemical forms of the weak acids need to be calculated.

2.1.1.1. Acid/base equilibrium. The equilibrium state of a solution containing several acid/conjugate base pairs and cations in known amounts can be computed by solving a system consisting in the following sets of equations:

2.1.1.1.1. Equations of conservation. The total amount of an acid is equal to the sum of the concentrations of all the ionic species formed by its dissociation:

$$\text{Citricacid} : [\text{Cit}] = [\text{H}_3\text{Cit}] + [\text{H}_2\text{Cit}^-] + [\text{HCit}^{2-}] + [\text{Cit}^{3-}] \quad (1a)$$

$$\text{Malicacid} : [\text{Mal}] = [\text{H}_2\text{Mal}] + [\text{HMal}^-] + [\text{Mal}^{2-}] \quad (1b)$$

$$\text{Oxalicacid} : [\text{Oxa}] = [\text{H}_2\text{Oxa}] + [\text{HOxa}^-] + [\text{Oxa}^{2-}] \quad (1c)$$

$$\text{Phosphoricacid} : [\text{PO}_4] = [\text{H}_3\text{PO}_4] + [\text{H}_2\text{PO}_4{}^-] + [\text{HPO}_4{}^{2-}] + [\text{PO}_4{}^{3-}] \quad (1d)$$

2.1.1.1.2. Equations of dissociation. The dissociation reactions of the weak acids considered in the model are the following:

$$\text{Citricacid} : \text{H}_3\text{Cit} \leftrightarrow \text{H}_2\text{Cit} + \text{H}^+ \leftrightarrow \text{HCit}^{2-} + 2\text{H}^+ \leftrightarrow \text{Cit}^{3-} + 3\text{H}^+ (\text{p}K\text{a}_1 \sim 3.10, \text{p}K\text{a}_2 \sim 4.70, \text{p}K\text{a}_3 \sim 6.40) \quad (2a)$$

$$\text{Malicacid} : \text{H}_2\text{Mal} \leftrightarrow \text{HMal}^- + \text{H}^+ \leftrightarrow \text{Mal}^{2-} + 2\text{H}^+ (\text{p}K\text{a}_1 \sim 3.40, \text{p}K\text{a}_2 \sim 5.10) \quad (2b)$$

$$\text{Oxalicacid} : \text{H}_2\text{Oxa} \leftrightarrow \text{HOxa}^- + \text{H}^+ \leftrightarrow \text{Oxa}^{2-} + 2\text{H}^+ (\text{p}K\text{a}_1 \sim 1.23, \text{p}K\text{a}_2 \sim 4.19) \quad (2c)$$

$$\text{Phosphoricacid} : \text{H}_3\text{PO}_4 \leftrightarrow \text{H}_2\text{PO}_4 + \text{H}^+ \leftrightarrow \text{HPO}_4{}^{2-} + 2\text{H}^+ \leftrightarrow \text{PO}_4{}^{3-} + 3\text{H}^+ (\text{p}K\text{a}_1 \sim 2.12, \text{p}K\text{a}_2 \sim 7.21, \text{p}K\text{a}_3 \sim 12.67) \quad (2d)$$

If HA/A^- is an acid/base pair characterized by an acidity constant K_a, the equilibrium between the concentrations of the protonated and the dissociated form can be written as a function of pH and of the activity of the ionic species involved in the reaction: $K_a = (A^-)h/(HA)$, where (HA) and (A^-) are the activities of the conjugated acid and base, respectively; $h = (H^+) = 10^{-\text{pH}}$ is the hydrogen ion activity, and $K_a = 10^{-\text{p}Ka}$ is the acidity constant.

In diluted solutions (concentrations below 10^{-2} mol L^{-1}), activities can be considered equal to concentrations. In more concentrated solutions like fruit juice, they are less than concentrations: $(HA) = a_{HA}[HA]$ and $(A^-) = a_A{-}[A^-]$, where $[HA]$ and $[A^-]$ are the concentrations of the acid and its corresponding base respectively, and a_{HA} and a_A- are the activity coefficients, which depend on the ionic composition of the solution. So, the dissociation equilibrium can be written by introducing an apparent acidity constant: $[A^-]h/[HA] = K'a$, where K'_a is the apparent constant of acidity defined as:

$$K'_a = K_a a_{HA}/a_{A^-} \quad (3)$$

2.1.1.1.3. Activity coefficient of ions. The activity coefficients of each acid and conjugated base have to be computed to estimate the apparent acidity constants. In a solution that contains n ionic species S_i with electric charges z_i and at concentrations $C_{i1<i<n}$, an ion S with a charge z has an activity coefficient a_s that depends on the ionic strength (μ) of the medium. The ionic strength of the solution is the total concentration in ionic species, given by the following equation:

$$\mu = 1/2\left(\sum_i z_i^2 C_i\right) \quad (4)$$

In the case of an aqueous solution with a ionic strength of up to 1 M, a_s can be calculated by the equation of Davies (1962):

$$\log(a_s) = -0.509z^2\left(\left(\sqrt{\mu}/(1+\sqrt{\mu})\right) - 0.3\mu\right) \quad (5)$$

2.1.1.1.4. Ionic balance. The neutrality of the electrical solution in pulp cell implies that the algebraic sum of cationic and anionic charged must be null:

$$[\text{H}_2\text{Cit}^-] + 2*[\text{HCit}^{2-}] + 3*[\text{Cit}^{3-}] + [\text{HOxa}^-] + 2*[\text{Oxa}^{2-}] + [\text{Hmal}^-] + 2*[\text{Mal}^{2-}] + [\text{H}_2\text{PO}_4{}^-] + 2*[\text{HPO}_4{}^{2-}] + 3*[\text{PO}_4{}^{3-}] + [\text{OH}^-] + [\text{Cl}^-] - [\text{H}^+] - [\text{K}^+] - 2*[\text{Mg}^{2+}] - 2*[\text{Ca}^{2+}] = 0 \quad (6)$$

$[\text{OH}^-]$ is expressed as a function of the pH: $[\text{OH}^-] = 10^{(\text{pH-14})}$

2.1.1.2. Algorithm of the pH model. Combinations of Eqs. (1) and (2) give the following set of equations that all depend on the apparent acidity constants and the pH:

$$[\text{Cit}^{3^-}] = (K'_{\text{cit}1}K'_{\text{cit}2}K'_{\text{cit}3}/(h^3 + h^2K'_{\text{cit}1} + hK'_{\text{cit}1}K'_{\text{cit}2} + K'_{\text{cit}1}K'_{\text{cit}2}K'_{\text{cit}3}))[\text{Cit}] \quad (7a)$$

$$[\text{HCit}^{2^-}] = (hK'_{\text{cit}1}K'_{\text{cit}2}/(h^3 + h^2K'_{\text{cit}1} + hK'_{\text{cit}1}K'_{\text{cit}2} + K'_{\text{cit}1}K'_{\text{cit}2}K'_{cit3}))[\text{Cit}] \quad (7b)$$

$$[\text{H}_2\text{Cit}^-] = (h^2K'_{\text{cit}1}/(h^3 + h^2K'_{\text{cit}1} + hK'_{\text{cit}1}K'_{\text{cit}2} + K'_{\text{cit}1}K'_{\text{cit}2}K'_{\text{cit}3}))[\text{Cit}] \quad (7c)$$

$$[\text{H}_3\text{Cit}] = (h^3/(h^3 + h^2K'_{\text{cit}1} + hK'_{\text{cit}1}K'_{\text{cit}2} + K'_{\text{cit}1}K'_{\text{cit}2}K'_{\text{cit}3}))[\text{Cit}] \quad (7d)$$

$$[Mal^{2-}] = (K'_{mal1}K'_{mal2}/(h^2 + hK'_{mal1} + K'_{mal1}K'_{mal2}))[Mal] \quad (7e)$$

$$[HMal^{-}] = (hK'_{mal1}/(h^2 + hK'_{mal1} + K'_{mal1}K'_{mal2}))[Mal] \quad (7f)$$

$$[H_2Mal] = (h^2/(h^2 + hK'_{mal1} + K'_{mal1}K'_{mal2}))[Mal] \quad (7g)$$

$$[Oxa^{2-}] = (K'_{oxa1}K'_{oxa2}/(h^2 + hK'_{oxa1} + K'_{oxa1}K'_{oxa2}))[Oxa] \quad (7h)$$

$$[HOxa^{-}] = (K'_{oxa1}/(h^2 + hK'_{oxa1} + K'_{oxa1}K'_{oxa2}))[Oxa] \quad (7i)$$

$$[H_2Oxa] = (h^2/(h^2 + hK'_{oxa1} + K'_{oxa1}K'_{oxa2}))[Oxa] \quad (7j)$$

$$[PO_4^{3-}] = (K'_{pho1}K'_{pho2}K'_{pho3}/(h^3 + h^2K'_{pho1} + hK'_{pho1}K'_{pho2} + K'_{pho1}K'_{pho2}K'_{hpo3}))[PO_4] \quad (7k)$$

$$[HPO_4^{2-}] = (hK'_{pho1}K'_{pho2}/(h^3 + h^2K'_{pho1} + hK'_{pho1}K'_{pho2} + K'_{pho1}K'_{pho2}K'_{hpo3}))[PO_4] \quad (7l)$$

$$[H_2PO_4^{-}] = (h^2K'_{pho1}/(h^3 + h^2K'_{pho1} + hK'_{pho1}K'_{pho2} + K'_{pho1}K'_{pho2}K'_{hpo3}))[PO_4] \quad (7m)$$

$$[H_3PO_4] = (h^3/(h^3 + h^2K'_{pho1} + hK'_{pho1}K'_{pho2} + K'_{pho1}K'_{pho2}K'_{hpo3}))[PO_4] \quad (7n)$$

So, combining Eqs. (3–7), it is possible to calculate the ionic strength (μ) and the pH of the pulp by solving a system of two equations with two unknowns (pH and μ).

$$F_1(\mu, \mathrm{pH}) = \sum \mathrm{Anions} - \sum \mathrm{Cations} = 0$$

$$F_2(\mu, \mathrm{pH}) = \mu - 1/2 \sum z_i^2[A_i] = 0$$

2.1.2. TA model

The TA of banana pulp was predicted by computing the amount of base (NaOH) needed to bring its pH to 8.1 (usual norm). Knowing the total concentrations of each acid and cation, and the pH of the pulp (equal to 8.1), it is possible to calculate the ionic strength (μ) and the TA of the pulp by solving a system of two equations with two unknowns (NaOH and μ):

$$F_1(\mu, \mathrm{NaOH}) = \sum \mathrm{Anions} - \sum \mathrm{Cations} = 0$$

$$F_2(\mu, \mathrm{NaOh}) = \mu - 1/2 \sum z_i^2[A_i] = 0$$

The input data of the model were the acid and cation concentrations of the banana pulp, and the acidity constants of the malic, citric, phosphoric and oxalic acid. The model was computed using R software (R Development Core Team, http://www.r-project.org). For each sampling date, the system was solved to calculate the pH of the pulp sample or the amount of NaOH added to reach a pH of 8.1, using the "nleqslv" function of the R software (http://cran.r-project.org/web/packages/nleqslv/index.html).

2.2. Model validation

2.2.1. Field experiment

Three dessert banana cultivars (Musa spp.) diploids AA, with different predominant organic acid at the eating stage were used in this study: Indonesia 100 (IDN 110), Pisang Jari Buaya (JB), and Pisang Lilin (PL). All bananas were grown at the *Pôle de Recherche Agroenvironnementale de la Martinique* (PRAM, Martinique, French West Indies; latitude 14°37 N, longitude 60°58 W, altitude 16 m) on continental alluvial soil.

Plants received 12 g of nitrogen, 1.7 g of phosphorus, and 20 g of potassium at 4-week intervals during fruit growth. Irrigation was adjusted to the amount of rainfall to supply at least 5 mm of water per day. The other cultural practices (desuckering, bunch management) were similar to those used in standard Cavendish production. During the period of bunch growth (March–November 2010) the mean daily temperature was 27 ± 1.2 °C. Non-systemic fungicide was applied during the experiment to control foliar diseases. For each cultivar, plants were tagged at inflorescence emergence. Bunches were not covered.

2.2.2. Preparation of samples

2.2.2.1. Monitoring fruit growth. Six bunches corresponding to six replicates of each cultivar were selected. One fruit located in the internal row of the second proximal hand was collected for analyses every 15 days. Sampling before natural ripening on standing plants, i.e. when the first yellow finger appears, determined the end of monitoring.

2.2.2.2. Monitoring postharvest fruit ripening. For each cultivar, six bunches were harvested between May and November 2011. For each cultivar, the harvest stage was calculated to be 70% of the flowering-to-yellowing time of the bunch on the tree. The second proximal banana hand per bunch was rinsed and dipped in fungicide (bitertanol, 200 mg L^{-1}) for 1 min. The fruits were placed in a plastic bag with 20 μm respiration holes and stored in boxes for 6 days at 18 °C. The fruits were then stored in a room at 18 °C and underwent ethylene treatment (1 mL L^{-1} for 24 h) to trigger the ripening process. After 24 h the room was ventilated and bananas were maintained at 18 °C for 13 days. A banana fruit was sampled at day 0 (before ethylene treatment), 3, 6, 9 and 13.

2.2.3. Chemical analyses

Pulp of the sampled fruit was freeze dried and mixed to obtain a dry powder. TA and pH were measured after dilution of 1 g of dry powdered banana pulp in 30 mL of distilled water. TA was determined by titration with NaOH (0.1 N) at pH 8.1 and expressed in milli-equivalents of acid (mEq) per 100 g of fresh weight (FW). Two analytical replicates per sample were performed for each analysis. Citric acid and malic acid were extracted with a mixture of solvents (methanol/water/chloroform) and purified with PVPP according to Gomez et al. (2007). Starting from initial conditions described by Bergmeyer (1983), enzymatic assays were adapted to be performed in each well of a 96 well Microplate using a robotic platform (Freedom EVO 75, *TECAN*) equipped with a microplate reader (Infinite 200, *TECAN*). All the following preparations were done for one microplate. Citric acid assay: a mixture was prepared containing 115 μg of malic acid dehydrogenase, 0.51 mg of lactate dehydrogenase and 5 mg of NADH in 12 mL of 0.6 mol L^{-1} glycylglycine buffer (pH 7.8). Then 100 μL of the mixture and 180 μL of extract or standard solution of citric acid (4–50 mg L^{-1}) were mixed in each well. Ten minutes later, absorbance was read at 340 nm (DO A) before 20 μL of citric acid lyase (6.4 U mL^{-1}) were added. The microplate was incubated for 3 h at room temperature and regularly shaken, before a second reading (DO B). Malic acid assay: a mixture was prepared with 6 mL of water and 6 mL of a

Table 1
Linear mixed model analyses of TA, pH, malic acid content, citric acid content, soluble oxalic acid content, and mineral content during fruit growth and fruit post harvest ripening in relation to fruit age and the three cultivars used in this study.

Parameter	Fruit stage	*F*-value and significance				
		t	*c*	t^2	t^3	*t*:*c*
TA	Growth	12.1***	126***	29.8***	7.0*	Ns
	Ripening	179***	73.6***	49.4***	4.4*	66.5***
pH	Growth	222***	69.9***	51.2***	Ns	16.0***
	Ripening	184***	64.4***	79.4***	Ns	46.2***
Citric acid content	Growth	602***	7.2**	Ns	Ns	20.7***
	Ripening	9.90**	93.1***	11.1**	5.1*	65.9***
Malic acid content	Growth	451***	98.4***	Ns	Ns	16.6***
	Ripening	220***	59.1***	126***	Ns	20.3***
Oxalic acid content	Growth	240***	24.5***	Ns	Ns	Ns
	Ripening	162***	10.5**	58.9***	13.2***	12.3***
K content	Growth	38.7***	20.6***	Ns	Ns	Ns
	Ripening	Ns	Ns	Ns	Ns	Ns
P content	Growth	66.6***	24.2***	Ns	Ns	Ns
	Ripening	Ns	47.0***	Ns	Ns	Ns
Cl content	Growth	76.0***	Ns	Ns	Ns	Ns
	Ripening	21.4***	8.5**	8.3**	Ns	Ns
Mg content	Growth	15.6**	5.1*	Ns	Ns	Ns
	Ripening	Ns	5.4*	Ns	Ns	Ns
Ca content	Growth	Ns	Ns	Ns	Ns	Ns
	Ripening	Ns	Ns	Ns	Ns	Ns

[a] All models included one random effect: "plant". Codes for effects: *t* = fruit age; *c* = cultivar.
Ns: not significant.
*** *p*-Value < 0.001.
** *p*-Value < 0.01.
* *p*-Value < 0.05.

0.6 mol L^{-1} glycylglycine buffer (pH 10). Then 100 μL of the mixture, 20 μL of NAD (18 mg mL^{-1}), 20 μL of GOT (66.7 mg L^{-1}) and 100 μL of extract or standard malic acid solution (4 to 50 mg L^{-1}) were mixed in each well. Ten minutes later, absorbance was measured at 340 nm (DO A) before 20 μL of malic acid dehydrogenase (33 μg mL^{-1}) were added. For the next 2 h 45 min, the microplate was incubated at room temperature and shaken twice, after which absorbance was measured at 340 nm (DO B). The concentration of soluble oxalic acid was determined using the LIBIOS Oxalic acid assay kit. Soluble K, Mg, and Ca concentrations were determined by mass spectrometry (Martin-Prével et al., 1984), and Cl concentration was determined by potentiometry using the automatic titrator TitroLine alpha (Walinga et al., 1995). The concentration of phosphoric acid was estimated from soluble phosphorus (P) determined by colorimetry (Martin-Prével et al., 1984).

2.2.4. Statistical analysis

Linear mixed-effects models [LMMs (Gałecki and Burzykowski, 2013)] were used to examine the relationship between the response variables (pulp acidity and composition) and the explanatory variables (fruit age, cultivar), and their interactions. We used quadratic and cubic terms of fruit age when the curve passed through a maximum and had an asymmetrical shape. We used the lme function in the 'nlme' library (Pinheiro et al., 2013) in the statistical program R 2.14.0. "Banana plant" was treated as a random effect because banana plants were assumed to contain unobserved heterogeneity that cannot be modeled. A temporal correlation structure was used to account for temporal pseudoreplication. Model selection was made using the top-down strategy (Zuur et al., 2009): starting with a model where the fixed component contains all explanatory variables and interactions, we found the optimal structure of the random component. Then, we used *F*-statistic obtained with REML estimation to find the optimal fixed structure. Finally, the optimal model is presented in this paper, using REML estimation.

The predictive quality of the pH and TA models was evaluated by the bias (mean of the difference between observed and predicted values), and the root mean squared error (RMSE), which describes the mean distance between simulation and measurement data (Kobayashi and Salam, 2000). The RMSE design was:

$$\mathrm{RMSE} = \sqrt{\frac{(\sum (yi_{\mathrm{p}}\text{-}yi_{\mathrm{m}})^2)}{n}}$$

where yi_{p} is the predicted value of the fruit *i*, and yi_{m} is the measured value of the fruit *i*. *n* is the data number.

A sensitivity analysis of the pH and TA models was performed at two different stages of fruit development- green (before ethylene treatment) and ripe (9 days after ethylene treatment), according to the method of Monod et al. (2006). First, border values of each of the eight input factors of the models were estimated as the extremes values of the dataset corresponding to the fruit stage considered for the sensitivity analysis. Then, for each input factor, their range of values was divided into five equal levels and a 5^8 factorial simulation design was created. Next, an analysis of variance (ANOVA) was performed on the model responses to study the contribution of each input factor to pH and TA variability. A sensitivity index (SI) of each input factor was calculated by dividing its sum of squares by the total sum of squares (Monod et al., 2006).

3. Results

3.1. Changes in pulp acidity

Fruit age and the cultivar had a significant effect on pH and TA during fruit growth (Table 1). Throughout fruit growth, PL had the most acidic fruits (TA = 3.5 mEq 100 g FW^{-1} ± 0.22; pH = 5.5 ± 0.13), IDN 110 fruits were intermediate (TA = 2.8 mEq 100 g FW^{-1} ± 0.31; pH = 5.7 ± 0.17), and JB had the least acidic fruits (TA = 2.3 mEq 100 g FW^{-1} ± 0.27; pH = 5.9 ± 0.28) (Fig. 1A and B). In all three cultivars, TA decreased slightly during the early stages of fruit growth and then increased slightly. pH increased throughout fruit growth in the three cultivars but most in JB.

Fruit age and the cultivar had a significant effect on pH and TA during post harvest fruit ripening (Table 1). The general patterns of TA and pH during post harvest ripening were similar in

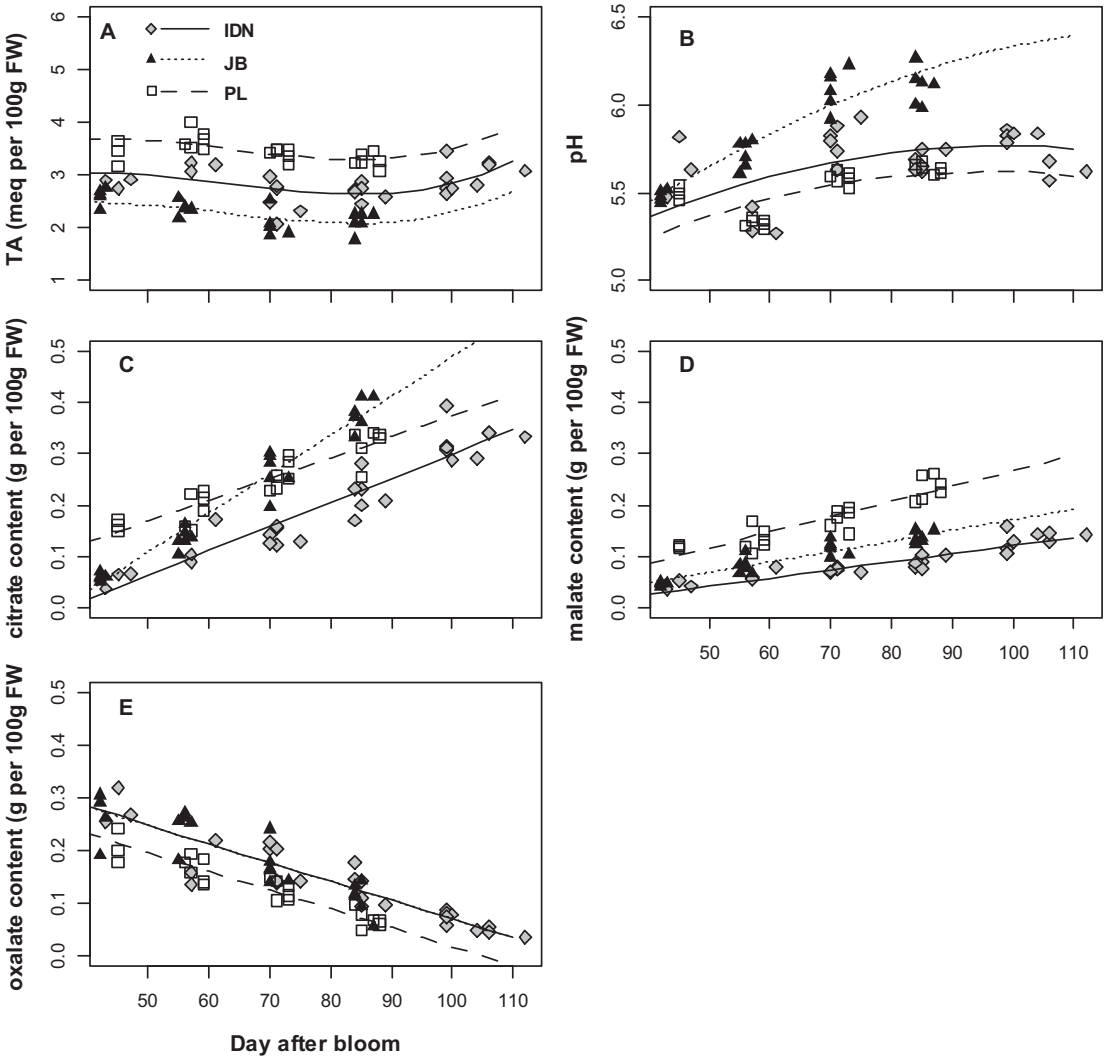

Fig. 1. Changes in TA (A), pH (B), citric acid content (C), malic acid content (D), and soluble oxalic acid content (E) of the pulp during fruit growth of the three cultivars of dessert bananas: Pisang Jari Buaya (JB), Pisang Lilin (PL), and Indonesia 110 (IDN 110). Each symbol represents a bunch. Lines are those of the fitted linear mixed model.

the three cultivars (Fig. 2A and B): TA increased from day 0 to day 6 and then decreased slightly until day 13. pH showed the opposite trend. There were strong significant differences between the three cultivars in the levels of TA and pH at the end of ripening (Fig. 2A and B). At day 13, JB had the highest acidity (TA = 12 mEq 100 g FW^{-1} ± 0.46; pH = 4.3 ± 0.05), followed by PL (TA = 6 mEq 100 g FW^{-1} ± 0.32; pH = 4.8 ± 0.08) and lastly IDN 110 (TA = 3.8 mEq 100 g FW^{-1} ± 0.43; pH = 5.4 ± 0.09).

3.2. Changes in organic acid and mineral contents

During fruit growth, citric and malic acid contents increased linearly in the three cultivars but at different rates leading to significant differences among cultivars (Fig. 1C and D, and Table 1).Thus, at the end of fruit growth, JB had the highest citric acid content (0.4 g 100 g FW^{-1} ± 0.03), followed by PL (0.34 g 100 g FW^{-1} ± 0.005) and IDN 110 (0.33 g 100 g FW^{-1} ± 0.001). Concerning malic acid content, PL had the highest content (0.23 g 100 g FW^{-1} ± 0.01) at the end of fruit growth, followed by JB (0.15 g 100 g FW^{-1} ± 0.003) and IDN 110 (0.14 g 100 g FW^{-1} ± 0.01). Soluble oxalic acid content decreased linearly during fruit growth in all three cultivars (Fig. 1E and Table 1). PL had a significantly lower soluble oxalic acid content than JB and IDN throughout fruit growth (Table 1). K was the main mineral present in banana pulp in the three cultivars and K content increased during fruit growth (Fig. 3A and Table 1). There were significant differences among cultivars (Table 1): JB had the highest K content (0.30 g 100 g FW^{-1} ± 0.02), followed by PL (0.26 g 100 g FW^{-1} ± 0.03), and IDN 110 (0.25 g 100 g FW^{-1} ± 0.02). The other mineral elements were present in lesser amounts (about ten times less) in banana pulp. Cl content increased from 0.05 to 0.07 g 100 g FW^{-1} during fruit growth and no differences were observed among the three cultivars whereas P content decreased during fruit growth in all three cultivars (Fig. 3B and C and Table 1). There were significant differences among cultivars throughout fruit growth and IDN 110 had a significantly higher P content (0.02 g 100 g FW^{-1} ± 0.002) than JB (0.01 g 100 g FW^{-1} ± 0.003) and PL (0.01 g 100 g FW^{-1} ± 0.003) (Fig. 3C and Table 1). Mg content decreased significantly during fruit growth in the three cultivars but most in PL (Fig. 3D and Table 1). Throughout fruit growth, JB (0.03 g 100 g FW^{-1} ± 0.001) and IDN 110 (0.03 g 100 g FW^{-1} ± 0.004) had a significantly higher Mg content than PL (0.02 g 100 g FW^{-1} ± 0.005). No clear pattern of Ca content was observed during fruit growth since the values varied greatly among bunches even within the same cultivar (Fig. 3E and Table 1).

During post harvest ripening, there were significant differences in the pattern of citric acid accumulation among the three cultivars (Fig. 2C and Table 1). Citric acid accumulation was the same in IDN 110 and PL with an overall decrease during ripening, whereas in JB

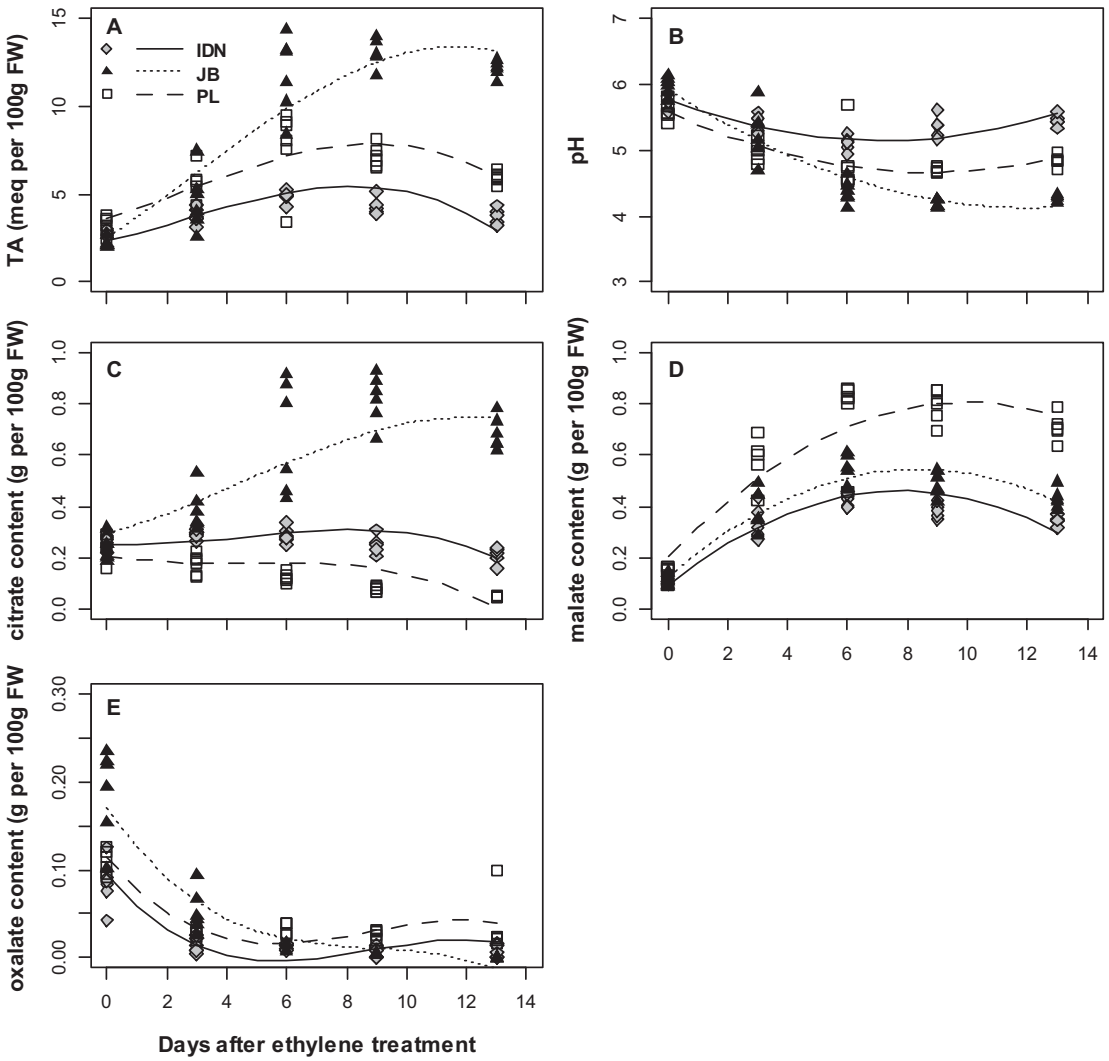

Fig. 2. Changes in TA (A), pH (B), citric acid content (C), malic acid content (D), and soluble oxalic acid content (E) of the pulp during post harvest ripening of the three cultivars of dessert bananas (JB, PL, and IDN 110). Each symbol represents a bunch. Lines are those of the fitted linear mixed model.

there was a significant increase until day 9 and a slight decrease at the end of ripening. As a consequence, JB had a significantly higher level of citric acid (0.68 g 100 g $FW^{-1} \pm 0.06$) than IDN 110 (0.21 g 100 g $FW^{-1} \pm 0.03$) and PL (0.05 g 100 g $FW^{-1} \pm 0.003$) at the end of ripening. The three cultivars showed the same pattern of malic acid accumulation with an increase from day 0 to day 6, followed by a slight decrease (Fig. 2D). There were significant differences among cultivars (Table 1), so that at the end of ripening, PL had the highest malic acid content (0.71 g 100 g $FW^{-1} \pm 0.05$), followed by JB (0.43 g 100 g $FW^{-1} \pm 0.04$) and IDN 110 (0.34 g 100 g $FW^{-1} \pm 0.02$). Soluble oxalic acid content was highest at the pre-climacteric stage (day 0) in all three cultivars with JB having a significantly higher oxalic acid content (0.19 g 100 g $FW^{-1} \pm 0.05$) than PL (0.14 g 100 g $FW^{-1} \pm 0.09$) and IDN 110 (0.08 g 100 g $FW^{-1} \pm 0.03$) (Fig. 2E and Table 1). From day 3, soluble oxalic acid content decreased rapidly in all three cultivars to become inexistent at the end of ripening. K was the main mineral found in banana pulp during post harvest ripening with a mean K content of 0.30 g 100 g $FW^{-1} \pm 0.05$ (Fig. 4A). K content remained constant during ripening and there were no significant differences among cultivars (Table 1). The other mineral elements such as Cl, Ca, Mg, and P were present in lower amounts (about ten times less) in the banana pulp. Cl content decreased slightly during ripening in all three cultivars and was significantly lower in PL (0.05 g 100 g $FW^{-1} \pm 0.006$) than in JB (0.07 g 100 g $FW^{-1} \pm 0.008$) and IDN 110 (0.06 g 100 g $FW^{-1} \pm 0.01$) (Fig. 4B and Table 1). P content remained constant during ripening in the three cultivars, IDN 110 had a significantly higher P content (0.02 g 100 g $FW^{-1} \pm 0.002$) than PL (0.01 g 100 g $FW^{-1} \pm 0.001$) and JB (0.01 g 100 g $FW^{-1} \pm 0.002$) (Fig. 4C and Table 1). Mg content remained constant during ripening in all three cultivars. PL had a significantly lower Mg content (0.02 g 100 g $FW^{-1} \pm 0.005$) than IDN 110 (0.03 g 100 g $FW^{-1} \pm 0.005$) and JB (0.03 g 100 g $FW^{-1} \pm 0.004$) (Fig. 4D and Table 1). There was no clear pattern in Ca content during fruit ripening since there was significant variability between bunches belonging to the same cultivar (Fig. 4E and Table 1).

3.3. Model predictions and sensitivity analysis

Overall, the pH model predicted banana pulp pH with an average bias of 0.05 pH units and a R^2 of 0.34 (Fig. 5A and B). The RMSE, quantifying the goodness-of-fit, was acceptable with a mean value of 0.7 pH unit (Table 2). However, the predictions were better for JB and PL than for IDN, and better during ripening than during fruit growth. For pH above 5, the discrepancies between observed and predicted values were sometimes higher than 1 pH unit. Overall, the TA model allowed prediction of banana pulp TA with an average bias of −1.44 mEq 100 g FW^{-1} and a R^2 of 0.81 (Fig. 5 C and D).

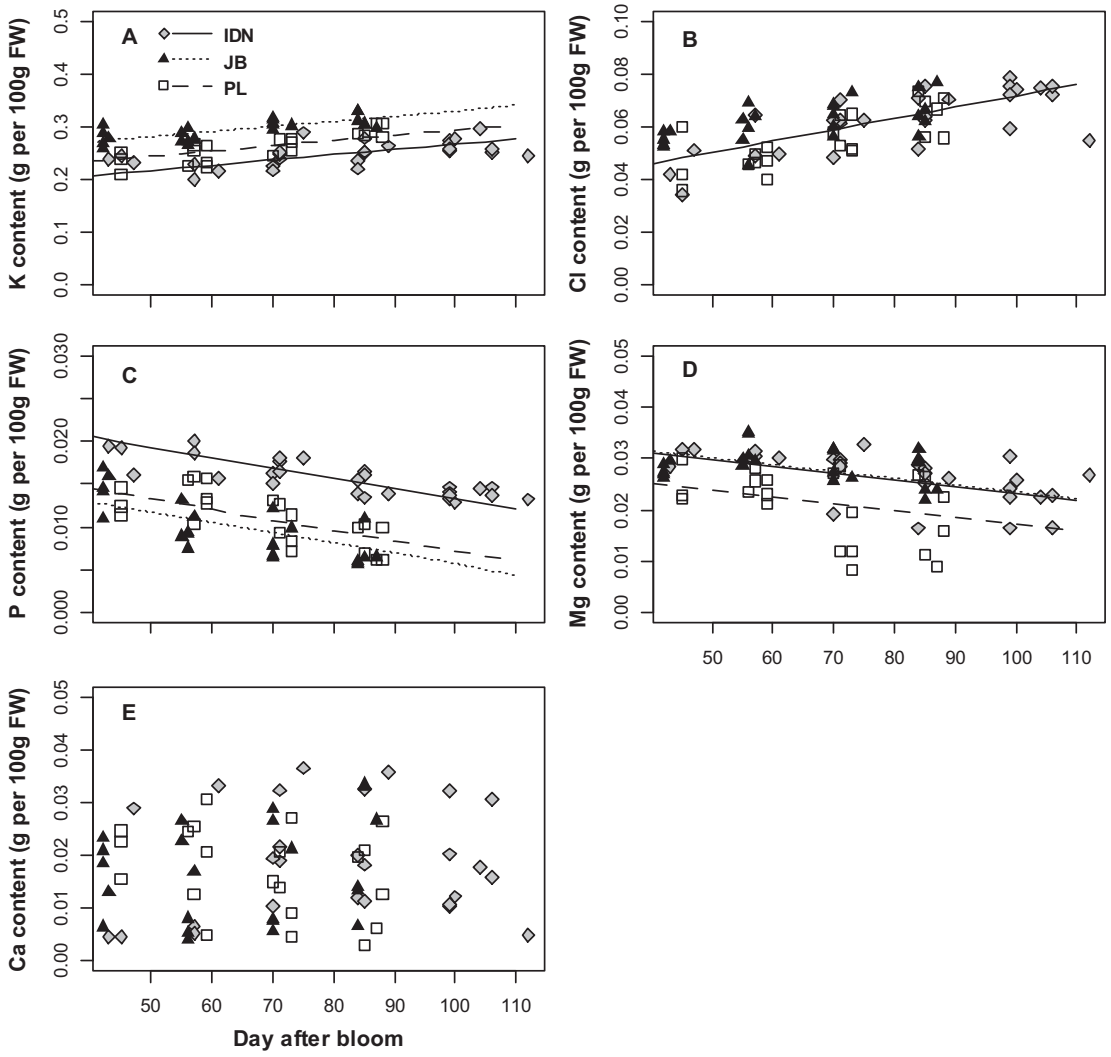

Fig. 3. Changes in K (A), Cl (B), P (C), Mg (D), and Ca (E) pulp content during fruit growth of the three cultivars of dessert bananas (JB, PL, and IDN 110). Each symbol represents a bunch. Lines are those of the fitted linear mixed model.

Thus, the model underestimated TA most of the time. The RMSE was satisfactory with a mean value of 2 mEq 100 g FW^{-1} (Table 2). The predictions were better during ripening than during fruit growth.

Every input factor considered in the sensitivity analysis had a significant effect on pH and TA at both green and ripe stages (Table 3). The sensitivity indices (SI) calculated represent the percentage of pH or TA variability explained by the factor considered. For both pH and TA, citric acid (SI = 48% for pH and 63% for TA) and malic acid (SI = 25% for pH and 21% for TA) were the most influential acids at the ripe stage, whereas phosphoric acid had little effect (SI = 5.6% for pH and TA), and oxalic acid had almost no effect (SI = 0.3% for pH and SI = 0.2% for TA). In contrast, at the green stage oxalic acid was the most influential acid (SI = 44% for pH and 48% for TA), whereas citric acid (SI = 4.5% for pH and 6.9% for TA), malic acid (SI = 0.9% for pH and 1.3 for TA), and phosphoric acid (SI = 0.5% for pH and TA) had very little effect. Among soluble minerals, K was the main contributor to changes in pH at both stages, but its effect was more pronounced at the green stage (SI = 39%) than at the ripe stage (SI = 14%). K was also the main contributor to TA at the green stage (SI = 37%), but its effect was greatly reduced at the ripe stage (SI = 6.9%). Other soluble minerals had only a limited effect on pH and TA since they accounted for a

Table 2
Quality of prediction (RMSE and bias) of the pH and TA models.

Cultivars	Fruit stage	pH		TA	
		RMSE (units pH)	Bias (units pH)	RMSE (mEq 100 g FW^{-1})	Bias (mEq 100 g FW^{-1})
PL	Growth	0.5	−0.2	1.5	−1.2
	Ripening	0.5	−0.1	2.6	−1.9
JB	Growth	0.6	0.1	1.3	−1.1
	Ripening	0.6	−0.2	2	−1
IDN 110	Growth	1	0.3	1.8	−1.5
	Ripening	1	0.4	2.4	−1.7
All cultivars	Growth	0.8	0.1	1.6	−1.3
	Ripening	0.7	0	2.3	−1.5
All cultivars	All stages	0.7	0.05	2	−1.4

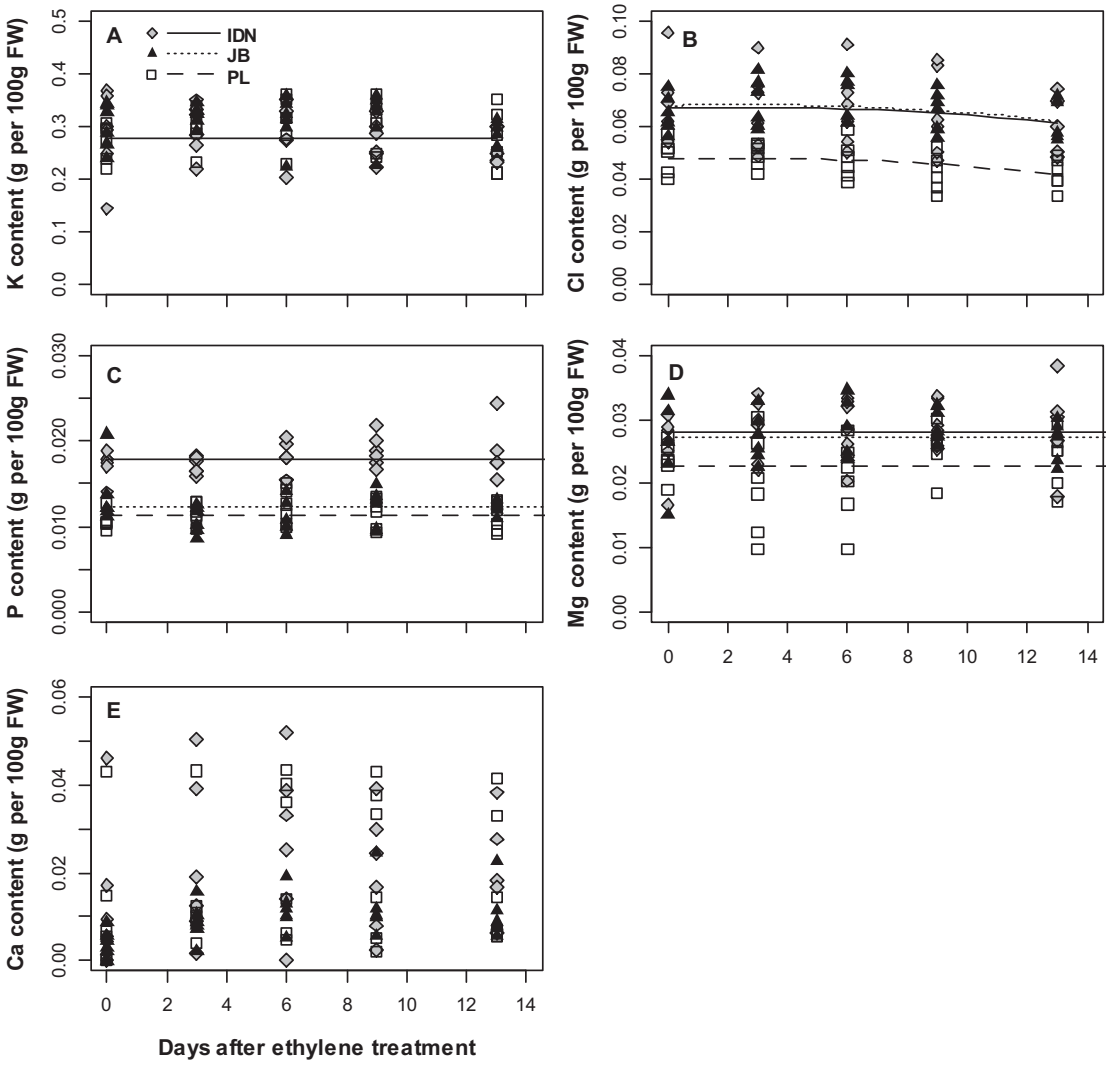

Fig. 4. Changes in K (A), Cl (B), P (C), Mg (D), and Ca (E) pulp content during post harvest ripening of the three cultivars of dessert bananas (JB, PL, and IDN 110). Each symbol represents a bunch. Lines are those of the fitted linear mixed model.

Table 3
Results of the sensitivity analysis of the pH and TA models for green (before ethylene treatment) and ripe fruits (9 days after ethylene treatment).

	Borders of the input factors		pH	TA
	Min. value (g 100 g FW^{-1})	Max. value (g 100 g FW^{-1})	SI (%)	SI (%)
		Ripe fruit		
Citric acid	0.04	1.02	48.4***	62.9***
Malic acid	0.05	0.93	25.6***	21.3***
Oxalic acid	0.00	0.19	0.28***	0.16***
Phosphoric acid	0.01	0.03	5.59***	5.64***
Potassium	0.13	0.43	13.9***	6.89***
Chloride	0.03	0.10	1.47***	0.71***
Magnesium	0.01	0.04	1.99***	0.99***
Calcium	0.00	0.05	2.76***	1.38***
		Green fruit		
Citric acid	0.05	0.41	4.55***	6.91***
Malic acid	0.04	0.35	0.96***	1.31***
Oxalic acid	0.02	0.29	43.7***	48.2***
Phosphoric acid	0.00	0.02	0.5***	0.55***
Potassium	0.22	0.33	39.3***	36.7***
Chloride	0.05	0.08	2.81***	2.80***
Magnesium	0.01	0.03	2.55***	2.59***
Calcium	0.00	0.04	5.84***	5.92***

The table gives the borders of the input factors, and the sensitivity indices (SI) with their significance.
*** p-Value < 0.001.

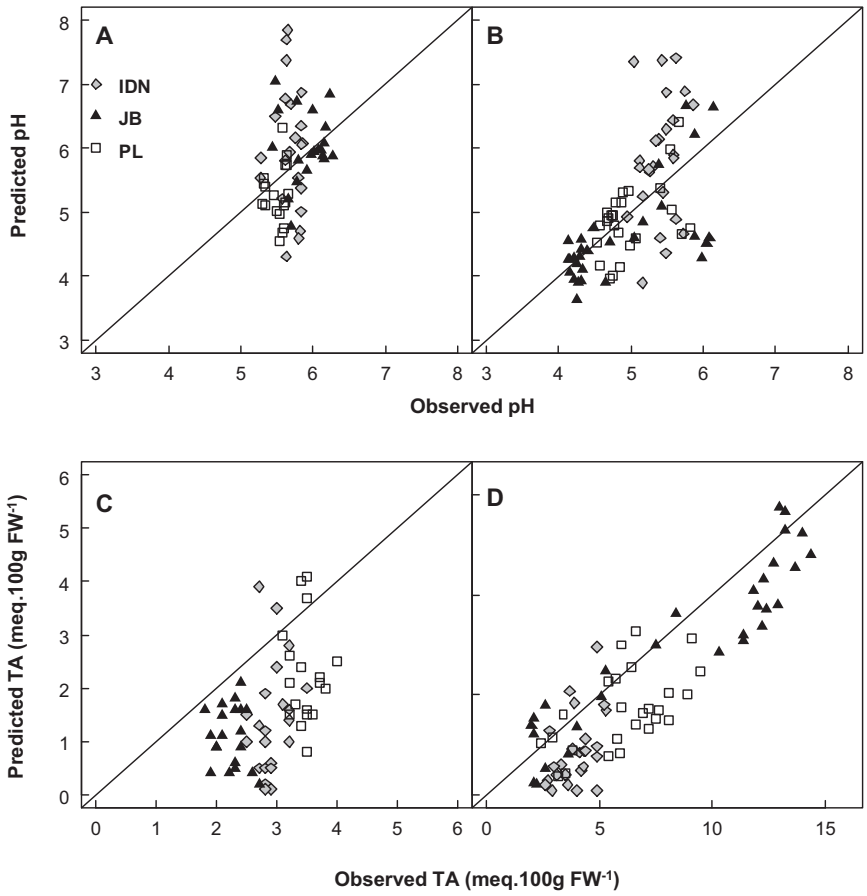

Fig. 5. Comparison between observed and predicted pH during fruit growth (A) and post harvest ripening (B), and between observed and predicted TA during fruit growth (C) and post harvest ripening (D) of the three cultivars of dessert bananas (JB, PL, and IDN 110).

total of 11% of their variability at the green stage and for a total of 6% and 3% for pH and TA respectively at the ripe stage.

4. Discussion

4.1. Quality of prediction of the models

For the pH model, the lower the pH, the better the predictions, which explains why pH predictions were better during ripening than during fruit growth. This is due to the logarithm function of the pH which increases the sensitivity of the pH to input parameters with an increase in pH. Thus, imprecision in the determination of the chemical elements that are the main contributors to banana pulp acidity (organic acids and K) may be responsible for the difference between observed and predicted data, especially at high pH. For example, we calculated that for a pulp sample with a measured pH of 6, overestimating the K content by 10% impacts the prediction by about 2 pH units. In addition, some approximations were used for modeling, for example, considering that all the soluble phosphorus is in the form of phosphoric acid whereas in reality it is probably also present in the form of several other acidic compounds than phosphoric acid. We also considered that the acid content of banana pulp could be estimated by malic acid, citric acid, oxalic acid and phosphoric acid content only. pH has been previously modeled using the same approach to predict acidity of ripe harvested peaches (Lobit et al., 2002). Predictions were a little better than those obtained in the present study which can be explained by the fact that pH of ripe peaches was below 4.5, and thus within the range where the model predictions are best.

For the TA model, predictions were on average 1.5 mEq lower than observed values. This is presumably because we did not consider free amino acids in the model and these can reach 0.1 g 100 g FW^{-1} and 0.15 g 100 g FW^{-1} in green and ripe bananas respectively (John and Marchal, 1995). Indeed, as the standard procedure is to measure TA at a pH of 8.1, not only carboxyl groups of amino acids are titrated but also some amine groups, probably leading to overestimation of the quantity of non-dissociated acids in fruit pulp. For ripe peaches, TA predictions were a little better than the ones obtained in the present study, probably due to the fact that amino acids were considered and approximated by the soluble nitrogen content of the pulp in the form of asparginine (Lobit et al., 2002). The authors calculated that at a pH of 8.1, free amino acids account for 8% of TA in ripe peach pulp. The better prediction of banana pulp TA during ripening was due to the fact that TA ranged from 3 to 15 mEq 100 g FW^{-1} during this stage, whereas it only varied between 2 and 4 mEq 100 g FW^{-1} during growth.

4.2. Link between banana pulp acidity and composition

The elaboration of banana fruit acidity is a continuous process that takes place throughout fruit growth and post harvest ripening. During its growth on the plant, the banana fruit accumulates both acids and minerals that determine the TA and pH of the pulp. Sensitivity analysis showed that during this phase, oxalic acid, which is present in large amounts, is the main determinant of banana pulp acidity because of its low p*K*as. Sensitivity analysis also showed that, among soluble minerals, K is the main contributor to banana acidity. K content increased during banana fruit growth, as also observed in mango (Léchaudel et al., 2005), and was the

major mineral found in banana pulp in accordance with results of previous studies (John and Marchal, 1995). It is interesting to note that K, which is the main cation present in all fruit cell, affects fruit acidity not only by participating in the acid/base reactions but also by acting on enzyme regulation and vacuolar storage of organic acids (Etienne et al., 2013).

During post harvest ripening, banana pulp acidity underwent its greatest changes and there were marked differences among the three cultivars. JB and PL appeared to have a higher acidity than IDN 110 at the end of ripening, which is in accordance with the classification of dessert bananas cultivars made by Bugaud et al. (2011). According to Bugaud's classification, JB and PL belonged to the sourest cluster whereas IDN 110 belonged to the least sour cluster. The marked changes in pulp acidity during post harvest ripening are mainly the result of changes in malic and citric acid contents as shown by the results of the sensitivity analysis. Indeed, as the fruit ripened, soluble oxalic acid content decreased dramatically, hence its contribution to banana fruit acidity. While oxalic acid disappears during ripening, malic and citric acids become the main acids in banana pulp and hence the main contributors to its acidity. The decrease in soluble oxalic acid content during banana fruit ripening is probably linked to starch hydrolysis. Indeed, Osuji and Ndukwu (2005) observed that oxalic acid was mainly present in the form of calcium oxalate crystals inside the starch grains in the pulp of unripe banana fruit. As the fruit ripened, the starch grains were destroyed and calcium oxalate released, probably leading to oxalate catabolism. The same pattern of oxalic acid content has been observed in kiwi fruit with a maximum at early stages and a gradual decrease during fruit growth and also during storage (Watanabe and Takahashi, 1998). The major role of malic and citric acids in the acidity of ripe fruit has been reported in many species (Etienne et al., 2013). Marked differences in the pattern of citric acid content were observed among the three cultivars. Thus, there was a significant increase in citric acid content in JB throughout fruit ripening while there was a decrease in PL and IDN 110. The pattern of malic acid content was the same in the three cultivars although differences were observed, with PL accumulating more malic acid than JB and IDN 110. Citric and malic acids are involved in the respiratory metabolism of fruit pulp cells through their involvement in the glycolysis and TCA cycle pathways (Etienne et al., 2013). As banana fruit, which is a climacteric fruit, showed a significant rise in their respiration rate in the first days after ethylene treatment, differences in pulp acidity among cultivars during ripening could be linked to respiratory metabolism. During post harvest ripening, K, P and Mg contents remained constant in all three cultivars, whereas Cl content decreased slightly. Migration of minerals from the pulp to the peel can occur in response to loss of water by the peel due to transpiration, but it is also possible that some minerals migrate with the water from the peel to the pulp (John and Marchal, 1995). In the present study, it appears that osmotic adjustment only significantly affected Cl content. There was a large variability of the soluble Ca content observed during ripening and growth but this is consistent with the high coefficient of variation of pulp Ca content that we found in previous studies. However, we showed that Ca did not play a major role in the determination of pH and TA, and so even if there was a large variability among samples in the measured Ca contents it did not have important repercussions on the predictions of the pH and TA models.

5. Conclusions

This study, which presents a model of banana pulp acidity for the first time, showed that among acids, malic, citric and oxalic acids are the main contributors to banana pulp acidity, and that among soluble minerals, K also plays an important role. Consequently, studying the factors that affect malic acid, citric acid, oxalic acid, and K accumulation in banana pulp appears to be an appropriate area of research to ultimately modify banana fruit acidity. In future work, the pH model will be incorporated in a more complex process-based simulation model to predict banana acidity. Process-based simulation models are powerful tools to study genotype*environment interactions and to design ideotypes adapted to consumer taste (Génard et al., 2010; Quilot-Turion et al., 2011).

Acknowledgment

Financial support for this study was provided by Structural European Funds.

References

Bergmeyer, H.U., 1983. Methods of Enzymatic Analysis. Verlag Chemie, Weinheim.
Bugaud, C., Cazevieille, P., Daribo, M.O., Telle, N., Julianus, P., Fils-Lycaon, B., Mbéguié-A-Mbéguié, D., 2013. Rheological and chemical predictors of texture and taste in dessert banana (*Musa* spp.). Postharvest Biol. Technol. 84, 1–8.
Bugaud, C., Deverge, E., Daribo, M.O., Ribeyre, F., Fils-Lycaon, B., Mbéguié-A-Mbéguié, D., 2011. Sensory characterisation enabled the first classification of dessert bananas. J. Sci. Food Agric. 91, 992–1000.
Chacón, S.I., Víquez, F., Chacón, G., 1987. Escala físico-química de maduración de banano. Physico-chemical banana ripening scale. Fruits 42, 95–102.
Davies, C.W., 1962. Ion Association. Butterworths, London.
Esti, M., Cinquanta, L., Sinesio, F., Moneta, E., Di Matteo, M., 2002. Physicochemical and sensory fruit characteristics of two sweet cherry cultivars after cool storage. Food Chem. 76, 399–405.
Etienne, A., Génard, M., Lobit, P., Mbeguié-A-Mbéguié, D., Bugaud, C., 2013. What controls fleshy fruit acidity? A review of malate and citrate accumulation in fruit cells. J. Exp. Bot. 64, 1451–1469.
Etxeberria, E., Pozueta-Romero, J., Gonzales, P., 2012. In and out of the plant storage vacuole. Plant Sci. 190, 52–61.
Gałecki, A., Burzykowski, T., 2013. Linear Mixed-Effects Model, Linear Mixed-Effects Models Using R. Springer, New York, 245-273.
Génard, M., Bertin, N., Gautier, H., Lescourret, F., Quilot, B., 2010. Virtual profiling: a new way to analyse phenotypes. Plant J. 62, 344–355.
Gomez, L., Bancel, D., Rubio, E., Vercambre, G., 2007. The microplate reader: an efficient tool for the separate enzymatic analysis of sugars in plant tissues—validation of a micro-method. J. Sci. Food Agric. 87, 1893–1905.
Izonfuo, W.-A.L., Omuaru, V.O.T., 1988. Effect of ripening on the chemical composition of Plantain peels and pulps (*Musa paradisiaca*). J. Sci. Food Agric. 45, 333–336.
John, P., Marchal, J., 1995. Ripening and biochemistry of the fruit. In: Gowen, S. (Ed.), Bananas and Plantains. Chapman and Hall, London, pp. 434–467.
Jullien, A., Chillet, M., Malezieux, E., 2008. Pre-harvest growth and development, measured as accumulated degree days, determine the post-harvest green life of banana fruit. J. Hortic. Sci. Biotechnol. 83, 506–512.
Kobayashi, K., Salam, M.U., 2000. Comparing simulated and measured values using mean squared deviation and its components. Agron J. 92, 345–352.
Léchaudel, M., Joas, J., Caro, Y., Génard, M., Jannoyer, M., 2005. Leaf:fruit ratio and irrigation supply affect seasonal changes in minerals, organic acids and sugars of mango fruit. J. Sci. Food Agric. 85, 251–260.
Lobit, P., Soing, P., Génard, M., Habib, R., 2002. Theoritical analysis of relationships between composition, pH, and titratable acidity of peach fruit. J. Plant Nutr. 25, 2775–2792.
Lyon, B.G., Robertson, J.A., Meredith, F.I., 1993. Sensory descriptive analysis of cv. Cresthaven peaches: maturity, ripening, and storage effects. J. Food Sci. 58, 177–181.
Madshus, I.H., 1988. Regulation of intracellular pH in eukaryotic cells. Biochem. J. 250, 1–8.
Martin-Prével, P., Gagnard, J., Gautier, P., 1984. L'analyse végétale dans le contrôle de l'alimentation des plantes tempérées et tropicales. Lavoisier, Paris.
Monod, H., Naud, C., Makowski, D., 2006. Uncertainty and Sensitivity Analysis for Crop Models. Elsevier, Amsterdam.
Osuji, J.O., Ndukwu, B.C., 2005. Probable functions and remobilisation of calcium oxalates in *Musa* L. Afr. J. Biotechnol. 4, 1139–1141.
Pinheiro, J., Bates, D., DebRoy, S., Sarkar, D., 2013. Package 'nlme': Linear and Nonlinear Mixed Effects Models.
Quilot-Turion, B., Ould-Sidi, M.M., Kadrani, A., Hilgert, N., Génard, M., Lescourret, F., 2011. Optimization of parameters of the 'Virtual Fruit' model to design peach genotype for sustainable production systems. Eur. J. Agron 42, 34–48.
Walinga, I., Lee, J., Houba, V., Vark, W.v., Novozamsky, I., 1995. Plant Analysis Manual. Kluwer Academic, Dordrecht.
Watanabe, K., Takahashi, B., 1998. Determination of soluble and insoluble oxalate contents in kiwifruit (*Actinidia deliciosa*) and related species. J. Jpn Soc. Hortic. Sci. 67, 299–305.
Zuur, A.F., Ieno, E.N., Walker, N., Saveliev, A.A., Smith, G.M., 2009. Mixed Effects Models and Extensions in Ecology with R. Springer, New York.